PHYSICAL REVIEW B **90**, 121301(R) (2014)

Excitation of complex spin dynamics patterns in a quantum-dot electron spin ensemble

S. Varwig,[1] I. A. Yugova,[2] A. René,[1] T. Kazimierczuk,[1] A. Greilich,[1] D. R. Yakovlev,[1,3] D. Reuter,[4] A. D. Wieck,[4] and M. Bayer[1,3]

[1]*Experimentelle Physik 2, Technische Universität Dortmund, 44221 Dortmund, Germany*
[2]*Spin Optics Laboratory, Saint-Petersburg State University, 198504 St. Petersburg, Russia*
[3]*Ioffe Physical-Technical Institute, Russian Academy of Sciences, 194021 St. Petersburg, Russia*
[4]*Angewandte Festkörperphysik, Ruhr-Universität Bochum, 44780 Bochum, Germany*

(Received 26 March 2014; revised manuscript received 15 August 2014; published 3 September 2014)

We exploit the flexibility offered by an (In,Ga)As/GaAs quantum dot spin ensemble to demonstrate that complex dynamic evolutions can be excited in the ensemble magnetization and accessed by tailored pulsed laser protocols. The modes for spin precession about a magnetic field are adapted to the periodic excitation protocol such that at specific times the magnetization can effectively be decomposed in two, three, or four equal components with angles of π, $2\pi/3$, or $\pi/2$ between them. Optical orientation of these components by an additional laser pulse leads to the generation of higher harmonics in the spin precession, as evidenced by time-resolved ellipticity measurements.

DOI: 10.1103/PhysRevB.90.121301 PACS number(s): 78.67.Hc, 78.20.Ls, 78.47.jm, 78.55.Cr

During recent years efficient tools for orientation and manipulation of spins in semiconductor quantum structures have been developed, employing optical pumping [1,2]. Because of the relevance for quantum information, most of these efforts focused on single spins in single quantum dots (QDs). Irrespective of the concrete implementation, these techniques exploit the polarization selection rules of the excited optical transitions [3]. To test the spin orientation, a transverse magnetic field may be applied about which the spins subsequently precess. The resulting spin dynamics are described by a simple harmonic function oscillating in time with the Larmor frequency. Experimental access to these dynamics can be obtained by Faraday rotation measurements [4,5].

Applying optical excitation protocols to ensembles of spins may give access to more complex dynamical evolutions due to the multiple degrees of freedom in the many-body system [6,7]. Nontrivial dynamics may arise from interactions between spins [8,9]. Also without interactions the ensemble response may be more intricate if the precession frequency distribution is inhomogeneously broadened [10]. While such inhomogeneities can be also deliberately introduced, they typically cannot be avoided during fabrication, in particular for self-assembled QD structures. These inhomogeneities in size, composition, etc., vary smoothly within a dot ensemble and translate into a corresponding variation of the confined spin properties such as the g factor, which is decisive for spin precession. The variation of g factors and therefore precession frequencies leads to a fast dephasing of the ensemble response even though spin coherence may be maintained [11].

The spin coherence can be retrieved from the dephased ensemble by applying specific laser excitation protocols. In the simplest form, periodic pulsed laser excitation is used, by which the spin dynamics become synchronized with the excitation: Due to the finite spectral width of the laser pulses, a distribution of precession frequencies is excited. If the frequencies are multiples of the laser repetition rate, the spins in these modes come into phase again at times around the pulse incidences, giving rise to a strong coherent signal [12,13]. This spin mode locking can be refined by varying, e. g., the magnetic field strength, the laser spectral width, or the pulse repetition rate, changing the distribution of the synchronized modes in the optically excited ensemble [10,14].

The potential offered by the inhomogeneity which on first sight may be considered as a disadvantage is somewhat similar to that in QD laser applications: For lasers it leads to a broad gain spectrum which may be favorably exploited for particular applications [15]. In any case, so far the ensemble spin dynamics has exhibited the (average) precession frequency of a single spin only, so that the dynamics has remained rather simple. Any possible flexibility from the ensemble has remained unexploited, for which multipulse excitation may be applied. Such excitation is well established in NMR [16,17], but studies using corresponding optical pulse sequences are still scarce [7,18,19].

Here we show that the excitation protocol can be adjusted such that the spin dynamics of an (In,Ga)As/GaAs QD ensemble is profoundly modified and higher harmonics are generated in the observed spin precession. For this demonstration we apply an additional excitation pulse, shifted together with the probe pulse, and exploit the inherent nonlinearity of QDs due to Pauli blocking to rectify the polarization of particular spin subsets, while leaving other spins' polarization unchanged. Thereby a modulated spin mode distribution is generated in the spin ensemble, as evidenced by the observation of double, triple, and quadruple precession frequencies in time-resolved ellipticity measurements. In effect, this method reveals spin-mode patterns which can be visualized as magnetization distributions with two, three, or four magnetization components of equal magnitude in the precession plane and angles of π, $2\pi/3$, or $\pi/2$, respectively, between them.

The experiments are performed on a sample containing 20 layers of (In,Ga)As QDs, decoupled by GaAs barriers. Si-doping sheets beneath each QD layer provide on average one resident electron per dot (see Ref. [20] for details). The ground state emission of the photoluminescence spectrum has its maximum at 1.393 eV and a full width at half maximum of 20 meV at $T = 6$ K temperature. All laser photon energies in the pump-probe experiments are tuned to this maximum.

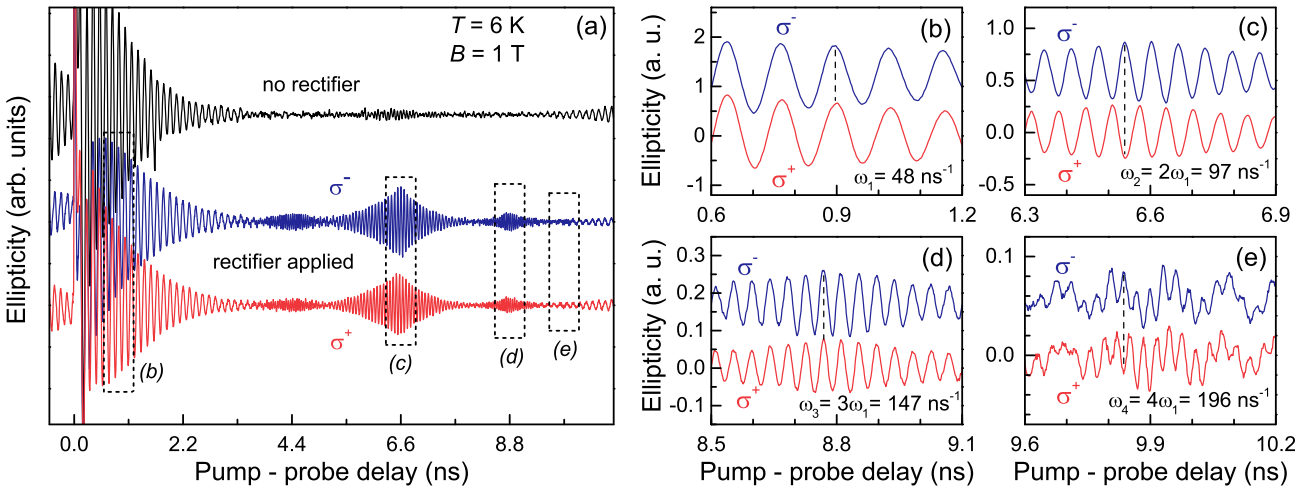

FIG. 1. (Color online) (a) Upper black curve: Ellipticity trace of QD spin ensemble excited by a train of pump pulses with separation $T_R = 13.2$ ns. $B = 1$ T and $T = 6$ K. Lower blue and red curves show ellipticities when an additional, circularly polarized (σ^- or σ^+, respectively) rectification pulse is applied, arriving at the sample simultaneously with the probe. Curves are shifted vertically for clarity. (b)–(e) Close-ups of the ellipticities with the rectifier applied for the 0.6-ns-delay ranges indicated by the boxes in (a). The observed precession frequencies are indicated in each panel. The slow oscillation in (e) superimposed on the signal is due to mode-locked spins while approaching the next pump pulse at 13.2 ns.

The resident electron spins in the QDs are oriented along the optical z axis by a train of circularly polarized pump pulses with a pulse area of π and a duration of about a picosecond, emitted with a repetition period of $T_R = 13.2$ ns. Subsequently the spins precess in the y-z plane about an external magnetic field, which is directed perpendicular to the optical axis along x. The overall spin polarization in the dot ensemble is determined by measuring the ellipticity acquired by linearly polarized probe pulses after transmission through the sample. The probe pulses are incrementally delayed relative to the pump pulses. The ellipticity changes are detected using balanced detection involving a lock-in technique by modulating the pump beam with a chopper.

An ellipticity measurement with the pump train only acting on the spins is shown by the top black curve in Fig. 1(a), recorded at $B = 1$ T for reference purposes. From the data the spin mode-locking achieved by the periodic excitation becomes obvious. After spin initialization at zero delay the spin precession shows a fast dephasing due to the g-factor inhomogeneities in the ensemble. However, the spins in precession modes locked to the laser repetition rate rephase before the next pump pulse excitation as evidenced by the ellipticity signal at delays <0 and $\gtrsim 10$ ns [12].

The lower blue and red curves in Fig. 1(a) show ellipticity measurements where the laser protocol is extended by an additional π pulse called "rectifier" (explained below), so that excitation by a pump doublet train is applied. The rectifier, either co- or countercircularly polarized relative to the pump, hits the sample at the same moment as the probe pulse. It is important to note that the rectifier is not modulated, so that the spin coherence induced by it is not detected after lock-in amplification, but only the rectifier's effect on the pump-induced coherence is seen. Adding the rectifier leads to the emergence of strong spin coherent signals at delays where the signal is completely dephased otherwise. These additional signals have maximum amplitudes at fractions of the separation between the pump pulses, namely, at $\frac{1}{4}T_R = 3.3$ ns, $\frac{1}{3}T_R = 4.4$ ns, $\frac{1}{2}T_R = 6.6$ ns, $\frac{2}{3}T_R = 8.8$ ns, and $\frac{3}{4}T_R = 9.9$ ns.

A closer look into these signals is taken in panels (b)–(e) of Fig. 1, showing close-ups for both circular polarizations of the rectifier. Panel (b) shows the spin dynamics following the pump at around 0.9 ns delay, demonstrating a precession frequency of $\omega_1 = 48$ ns^{-1}, basically identical to the situation without rectifier. The precession phase is not influenced by the rectifier's helicity as indicated by the dashed line. This is different for the range around $\frac{1}{2}T_R = 6.6$ ns in panel (c). Here, the precession frequency is doubled and the signals are in counterphase for the two different rectifier polarizations. In panel (d) the ellipticity around $\frac{2}{3}T_R = 8.8$ ns is found to oscillate at the threefold frequency compared to (a) without a phase change between σ^+ and σ^- rectifier polarization. A similar signal pattern is observed around $\frac{1}{3}T_R = 4.4$ ns. Finally, panel (e) shows the range around $\frac{3}{4}T_R = 9.9$ ns where—besides some signal contributions from mode-locked spins—a frequency component four times higher than the original one is observed, whose phase switches with the rectifier polarization. Quadruple frequencies occur also around $\frac{1}{4}T_R = 3.3$ ns.

To understand the oscillations with multifold frequencies one has to consider the distribution of mode-locked electron spins. Their precession frequencies ω fulfill the relation [12]

$$\omega = N\frac{2\pi}{T_R}, \tag{1}$$

with N being an integer. Figure 2(a) shows schematically the precession of the modes with the six lowest precession frequencies ($N = 1, \ldots, 6$) fulfilling Eq. (1). These modes were chosen for demonstration purposes: The single spin Larmor frequency at $B = 1$ T, $\omega_1 = 48$ ns^{-1}, corresponds to slightly more than 100 precessions between two pump pulses. For the applied laser pulses with a spectral width of about

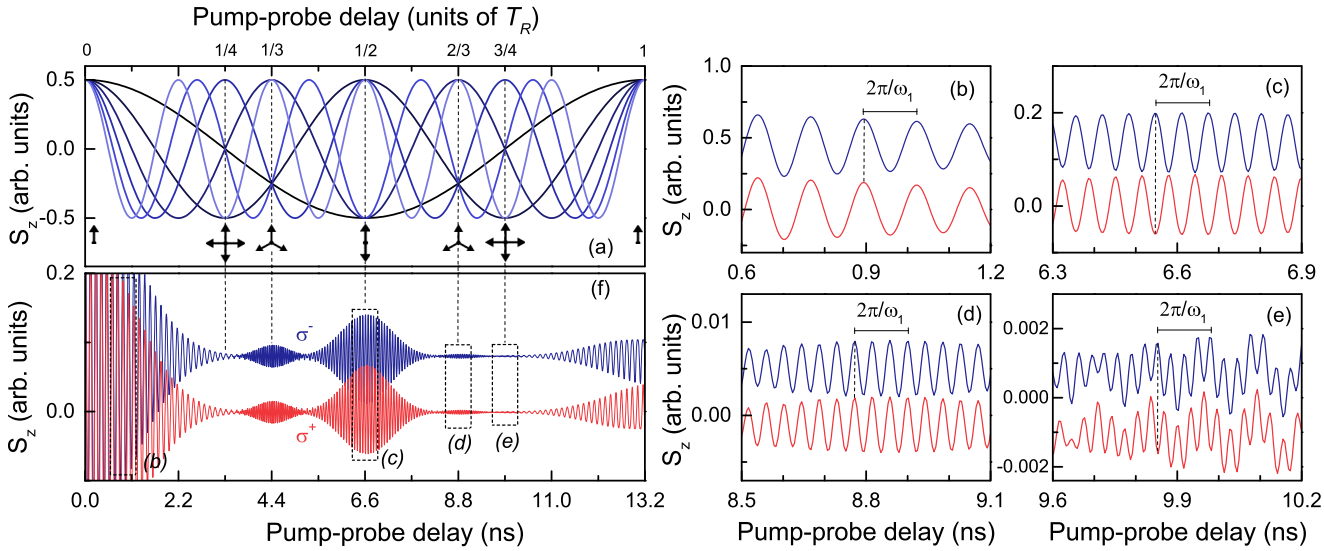

FIG. 2. (Color online) (a) Precession of the six lowest frequency modes fulfilling Eq. (1). At zero delay all spins point along $+z$ due to the pump action, illustrated by the single arrow. At $\frac{1}{4}T_R = 3.3$ ns and $\frac{3}{4}T_R = 9.9$ ns one-quarter of the spins each point along $+z$, $-z$, $+y$, and $-y$. At $\frac{1}{3}T_R = 4.4$ ns and $\frac{2}{3}T_R = 8.8$ ns the spins point, equally distributed, in one of three directions, separated by 120° as indicated by the arrow pattern. At $\frac{1}{2}T_R = 6.6$ ns half of the spins point along $+z$, and the other half along $-z$. (b)–(f) Modeled electron spin polarization S_z for both circular polarizations of the rectifier. Curves are vertically shifted for clarity. The parameters used in the calculations are $|g| = 0.56$, $\Delta g = 0.01$, $T_R = 13.2$ ns, and $B = 1$ T.

1 meV, around ten of such modes are excited [see the mode spectrum calculated for π-pulse excitation in Fig. 3(a).] There, the z component of the spin polarization is shown for the moment of pump action at zero delay.

Nevertheless, from the simple representation in Fig. 2(a) it becomes clear that at arbitrary delays the spin system is disordered reflecting the dephasing. However, at the times when higher harmonics are observed, the mode-locked spins form particular magnetization patterns: At $\frac{1}{2}T_R = 6.6$ ns in between two pump pulses, half of the mode-locked spins point along $+z$ while the other half points along the $-z$ direction, as indicated by the double arrow in Fig. 2(a). Furthermore, also at $\frac{1}{3}T_R = 4.4$ ns and $\frac{2}{3}T_R = 8.8$ ns ordered spin patterns are formed by three effective spins with an angle of 120° between them (see the arrow patterns). Finally, at $\frac{1}{4}T_R = 3.3$ ns and $\frac{3}{4}T_R = 9.9$ ns one-quarter of the spins each points along $+z$, $-z$, $+y$, and $-y$. At these delays the spin ensemble also forms a well-ordered pattern, but the net magnetization is zero.

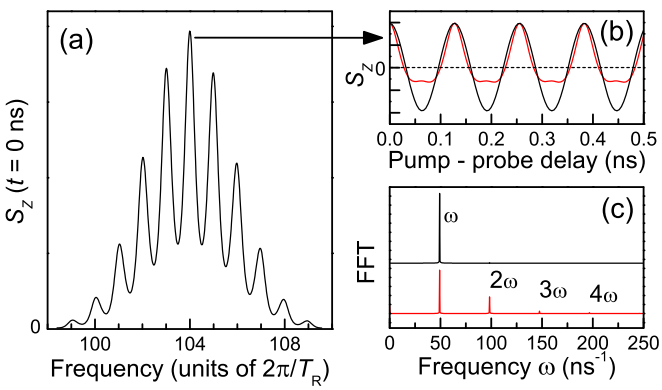

FIG. 3. (Color online) (a) Precession frequency mode spectrum simulated for zero delay at $B = 1$ T with only the pump applied. (b) Time evolution for the most pronounced precession mode with $\omega = 104 \times 2\pi/T_R$ for two cases: without the rectifier (black) and with the rectifier (red). (c) Fourier transforms of the time evolutions for both cases of panel (b).

Access to these spin patterns is granted, if together with the linearly polarized probe the circularly polarized rectification pulse hits the sample. This rectifier introduces an imbalance in the spin patterns, exploiting the nonlinearity provided by Pauli blocking. Pauli blocking prevents excitation of an electron spin with orientation parallel to the resident one. This has profound consequences. The precessing spins are superposition states of spin up and spin down. Assuming a σ^--polarized rectifier, an electron-hole pair with electron spin up (along $+z$) would be added to the already existing spin polarization. However, this is possible only for spin superposition states containing a downward ($-z$) component. Their spin-up part remains unexcited while the spin-down component is excited to a charged exciton complex with two electrons in a singlet state, not contributing to the magnetization. Thus, a spin-down state is knocked off from its contribution to the ensemble spin polarization, from which the pulse denomination rectifier is derived. As a consequence of this rectification the spectrum of mode-locked electron spins becomes modified. Note that the rectifier pulse does not create any new spin coherence, but manipulates only the existing one. As its photon energy is resonant with the pump pulse and its pulse area is set to π, the rectifier also does not introduce any spin rotation [21].

For a more quantitative description, we consider resonant excitation of the trion complex by a π pulse for simplicity [22]. The action of the π pulse has the following impact on the electron spin polarization:

$$S_z^a = \mp\tfrac{1}{4} + \tfrac{1}{2}S_z^b, \quad S_y^a = 0\,, \tag{2}$$

where the superscripts a and b denote the spin components after and before the pulse action, respectively. The top (bottom) sign $-$ $(+)$ corresponds to σ^+ (σ^-) polarized pump pulses.

After pump action at time $t = 0$ spin precession about the magnetic field starts, so that

$$\begin{aligned} S_z(t) &= S_z^a \cos(\omega t) + S_y^a \sin(\omega t), \\ S_y(t) &= -S_z^a \sin(\omega t) + S_y^a \cos(\omega t). \end{aligned} \tag{3}$$

Here we neglect contributions of the trion recombination to the spin polarization of the resident electrons, which is justified by the strength of the applied magnetic field, at which the hole precession annihilates any trion contribution. We also neglect any effects from transverse spin relaxation of electrons, because the corresponding spin coherence time T_2 is about two orders of magnitude longer than the pulse separations [12].

This spin polarization is modified by the rectification pulse, whose impact is also described by Eq. (2). For the rectifier pulse we also assume an area of π. The effect on the pump-induced spin coherence is shown in more detail in Fig. 3(b), where the black reference curve shows the precession of a spin belonging to the central precession mode in Fig. 3(a) with $N = 104$ after pump action only. The red curve, on the other hand, shows the impact of the rectifier that is shifted together with the probe. Obviously its action corresponds to a rectification, because the negative spin polarization cycles are in effect cut off. From this evolution, it is evident that the signal contains not only the fundamental Larmor frequency but also higher frequency components.

After an infinite train of pump-rectifier doublets the spin components just before rectifier arrival have the form (for details see Refs. [12,23,24])

$$\begin{aligned} S_z^{b*} &= \mp\frac{\Delta}{16}\{4\cos(\omega T_D) + \cos[2\omega(T_D - T_R/2)] \\ &\quad + \cos(\omega T_R)\}, \\ S_y^{b*} &= \pm\frac{\Delta}{16}\{4\sin(\omega T_D) + \sin[2\omega(T_D - T_R/2)] \\ &\quad + \sin(\omega T_R)\}, \\ \Delta &= \frac{1}{1 - \frac{1}{8}\{\cos[2\omega(T_D - T_R/2)] + \cos(\omega T_R)\}} \\ &\approx 1 + \frac{1}{8}\{\cos[2\omega(T_D - T_R/2)] + \cos(\omega T_R)\}, \end{aligned} \tag{4}$$

where the last approximation can be made because the two cosine terms are considerably smaller than unity. Again the top (bottom) sign $-$ $(+)$ corresponds to σ^+ (σ^-) polarized pulses. The multiplication of the harmonic functions leads to precession terms with the fundamental frequency ω_1 as well as the double, triple, and quadruple frequencies.

After averaging S_z over the Larmor frequency spread, these terms result in strong coherent signals at $\frac{1}{4}T_R$, $\frac{1}{3}T_R$, $\frac{1}{2}T_R$, $\frac{2}{3}T_R$, and $\frac{3}{4}T_R$ delays. Only around these delays the harmonic terms interfere constructively, because at these moments there is an order in the ensemble set by the pump pulse as shown by the sketches in Fig. 2(a). Generally the times of strong coherent signals $T_D = T_R/M$ are given by the delay between two pumps T_R being a multiple of the delay between pump and rectifier T_D. At these delays the rectification leads to a spin-coherent signal with a frequency which is M times the single spin Larmor precession frequency. Here, M determines the fraction $1/M$ of spins that are parallel to the z direction.

The results of detailed calculations are shown in Figs. 2(b)–2(f). The signals for co- and counterpolarized rectifiers are in good accord with the experiment. The smaller amplitudes of bursts at $\frac{2}{3}T_R$ and $\frac{3}{4}T_R$, as compared with the experiment in Fig. 1, may be due to the fact that nuclear effects, which lead to frequency focusing [25], were not considered theoretically.

In summary, we have demonstrated that QD spin ensembles offer interesting and flexible possibilities for generating complex spin dynamics. In our case this flexibility is provided by the inhomogeneity from the fabrication. This inhomogeneity can be adjusted, however, by tailored laser excitation protocols. The spin dynamics could be used to generate higher harmonics in the spin precession. We expect that by further elaboration of laser excitation, appealing spin dynamics may be generated through shaping the spin precession mode distribution exploiting degrees of freedom such as amplitude and phase of particular modes within the ensemble. Doing so, the ensemble spin dynamics can be flexibly modified by reprogramming the excitation sequence.

This work was supported by the Deutsche Forschungsgemeinschaft (DFG) and the BMBF project Q.com-H. M.B. acknowledges support from the Russian Ministry of Science and Education (Contract No. 14.Z50.31.0021).

[1] *Optical Generation and Control of Quantum Coherence in Semiconductor Nanostructures*, edited by G. Slavcheva, and P. Roussignol (Springer-Verlag, Berlin, 2010).

[2] A. J. Ramsey, Semicond. Sci. Technol. **25**, 103001 (2010).

[3] *Semiconductor Quantum Bits*, edited by F. Henneberger, and O. Benson (Pan Stanford, Singapore, 2008).

[4] *Semiconductor Spintronics and Quantum Computation*, edited by D. D. Awschalom, D. Loss, and N. Samarth (Springer-Verlag, Heidelberg, 2002).

[5] *Spin Physics in Semiconductors*, edited by M. I. Dyakonov (Springer-Verlag, Berlin, 2008).

[6] Y. Shen, A. M. Goebel, and H. Wang, Phys. Rev. B **75**, 045341 (2007).

[7] E. A. Zhukov, D. R. Yakovlev, M. M. Glazov, L. Fokina, G. Karczewski, T. Wojtowicz, J. Kossut, and M. Bayer, Phys. Rev. B **81**, 235320 (2010).

[8] V. V. Dobrovitski, A. E. Feiguin, D. D. Awschalom, and R. Hanson, Phys. Rev. B **77**, 245212 (2008).

[9] S. Spatzek, A. Greilich, S. E. Economou, S. Varwig, A. Schwan, D. R. Yakovlev, D. Reuter, A. D. Wieck, T. L. Reinecke, and M. Bayer, Phys. Rev. Lett. **107**, 137402 (2011).

[10] A. Greilich, M. Wiemann, F. G. G. Hernandez, D. R. Yakovlev, I. A. Yugova, M. Bayer, A. Shabaev, Al. L. Efros, D. Reuter, and A. D. Wieck, Phys. Rev. B **75**, 233301 (2007).

[11] I. A. Yugova, A. Greilich, E. A. Zhukov, D. R. Yakovlev, M. Bayer, D. Reuter, and A. D. Wieck, Phys. Rev. B **75**, 195325 (2007).

[12] A. Greilich, D. R. Yakovlev, A. Shabaev, Al. L. Efros, I. A. Yugova, R. Oulton, V. Stavarache, D. Reuter, A. D. Wieck, and M. Bayer, Science **313**, 341 (2006).

[13] S. G. Carter, A. Shabaev, Sophia E. Economou, T. A. Kennedy, A. S. Bracker, and T. L. Reinecke, Phys. Rev. Lett. **102**, 167403 (2009).

[14] A. Greilich, S. Spatzek, I. A. Yugova, I. A. Akimov, D. R. Yakovlev, Al. L. Efros, D. Reuter, A. D. Wieck, and M. Bayer, Phys. Rev. B **79**, 201305(R) (2009).

[15] *Lasers Based on Quantum Dot Structures: Physics and Devices*, edited by E. U. Rafailov (Wiley-VCH, Weinheim, 2011).

[16] A. Abragam, *Principles of Nuclear Magnetism* (Oxford University Press, New York, 1961).

[17] J. Du, X. Rong, N. Zhao, Y. Wang, J. Yang, and R. B. Liu, Nature (London) **461**, 1265 (2009).

[18] D. Press, T. D. Ladd, B. Zhang, and Y. Yamamoto, Nature (London) **456**, 218 (2008).

[19] S. Varwig, A. René, S. E. Economou, A. Greilich, D. R. Yakovlev, D. Reuter, A. D. Wieck, T. L. Reinecke, and M. Bayer, Phys. Rev. B **89**, 081310(R) (2014).

[20] A. Greilich, R. Oulton, E. A. Zhukov, I. A. Yugova, D. R. Yakovlev, M. Bayer, A. Shabaev, Al. L. Efros, I. A. Merkulov, V. Stavarache, D. Reuter, and A. Wieck, Phys. Rev. Lett. **96**, 227401 (2006).

[21] A. Greilich, S. E. Economou, S. Spatzek, D. R. Yakovlev, D. Reuter, A. D. Wieck, T. L. Reinecke, and M. Bayer, Nat. Phys. **5**, 262 (2009).

[22] I. A. Yugova, M. M. Glazov, E. L. Ivchenko, and Al. L. Efros, Phys. Rev. B **80**, 104436 (2009).

[23] I. A. Yugova, M. M. Glazov, D. R. Yakovlev, A. A. Sokolova, and M. Bayer, Phys. Rev. B **85**, 125304 (2012).

[24] See Supplemental Material at http://link.aps.org/supplemental/10.1103/PhysRevB.90.121301 for a more detailed view on the theoretical model and comparisons with the experiment.

[25] A. Greilich, A. Shabaev, D. R. Yakovlev, Al. L. Efros, I. A. Yugova, D. Reuter, A. D. Wieck, and M. Bayer, Science **317**, 1896 (2007).